

2-(2,3,4,5,6-Pentafluorophenyl)-1*H*-benzo[*d*]imidazole, a fluorine-rich building block for the preparation of conjugated polymer donors for organic solar cell applications†

Marios Neophytou,^a Heraklidia A. Ioannidou,^b Theodosia A. Ioannou,^{ab} Christos L. Chochos,^a Solon P. Economopoulos,^a Panayiotis A. Koutentis,^b Grigorios Itskos^c and Stelios A. Choulis^{*a}

Received 6th April 2012, Accepted 2nd May 2012

DOI: 10.1039/c2py20198d

We have introduced the pentafluorophenyl substituted benzimidazole as a building block of conjugated polymers for optoelectronic applications. We present the synthesis of a copolymer bearing fluorene as the comonomer. A detailed characterization of the novel material including structural, electrochemical and optical (using absorption, emission and time-resolved photoluminescence techniques) properties as well as computational modeling is described. The polymer exhibits highly efficient photoluminescence quenching when blended with fullerene derivatives (PCBM). The experimental results are compared with the alternating fluorene copolymer (APFO-3) in order to identify structure and property relations with the novel synthesized conjugated polymer. Early photovoltaic performance data are presented and compared with the well established APFO-3 : PCBM material system.

Introduction

The research area of polymer–fullerene bulk heterojunction solar cells¹ has witnessed a rapid growth in the efficiency of the cells over the last 5 years and state of the art organic solar cells currently have power conversion efficiencies close to 10%,^{2–5} with a 9.1% efficiency very recently reported by Polyera.⁶ Throughout the community, one of the main interests, from a chemical perspective, lies in the synthesis of new electron donor solar absorbers, since fullerene and its soluble derivatives^{7–9} are currently considered as the electron acceptors of choice. As a synthetic guideline, several key aspects of the polymer have to be chemically tailored to obtain an attractive material for optoelectronic applications. The synthetic efforts to create new electron donor polymers were guided by the following desired attributes of the material: (1) broad absorption covering most of the visible light range and extending to the near-IR range up to the predicted optimum gap for single-junction cells of 1.1 μm .¹⁰ (2) High hole mobilities for efficient charge transport with values within an optimum range matching the electron mobilities in the fullerenes and (3) optimum energy level spacing allowing for efficient electron transfer to the fullerene with minimum losses to

thermal energy, while minimizing the energy barrier to the charge-collecting electrodes.

Fluorine has received great attention in materials science owing to the interesting variations of the properties of materials with fluorine incorporated into the structure.¹¹ Its uses range from the well-studied Teflon® and other fluorinated polymers^{12–15} to more recent materials, such as, fluoro-graphene.^{16,17} The effects induced by fluorine addition in organic molecules include, among others, high oxidative stability¹⁸ and degradation resistance.¹⁹ There are examples of fluorinated oligomers and polymers that have applications in organic light emitting diodes,^{20,21} as well as field effect transistors.^{22–24} The fluorine atom being the most electronegative element is expected to stabilize the lowest unoccupied and the highest occupied molecular orbitals, LUMO and HOMO, respectively, upon incorporation into conjugated polymers. Moreover, concerning conjugated polymers, there is an established notion that a weak donor–strong acceptor copolymerization approach can yield desirable optoelectronic characteristics in the end-material.^{25–27} As fluorine can enhance the electronegativity of a given moiety, the use of fluorinated analogues in organic solar cells has led to enhanced power conversion efficiencies.^{2,3,28–30}

Based on the above considerations, we synthesized a novel benzo[*d*]imidazole³¹ monomer that was functionalized with perfluorophenyl to improve its acceptor character, and then polymerized this with an electron donor comonomer. As compared to benzo[1,2,5]thiadiazole, benzo[1,2,5]selenadiazole, benzo[1,2,5]-oxadiazole and benzo[*d*][1,2,3]triazole, benzo[*d*]imidazole is the less explored member of this homologue family. Recently, Suh *et al.* examined the properties and the primary photovoltaic

^aMolecular Electronics and Photonics Research Unit, Department of Mechanical Engineering and Materials Science and Engineering, Cyprus University of Technology, 3603 Limassol, Cyprus

^bDepartment of Chemistry, University of Cyprus, P.O. Box 20537, 1678 Nicosia, Cyprus

^cExperimental Condensed Matter Physics Laboratory, Department of Physics, University of Cyprus, P.O. Box 20537, 1678 Nicosia, Cyprus

† Electronic supplementary information (ESI) available. See DOI: 10.1039/c2py20198d

performance of several dialkyl substituted 2*H*-benzo[*d*]imidazole-based conjugated polymers,³² while the initial properties of alternating copolymers based on alkyl-substituted 1*H*-benzo[*d*]imidazole have been presented by Yamamoto and Hayashi.³³ More recently, a study on blue light emitters using benzimidazole and fluorene copolymers was published, denoting interest in this class of materials.³⁴

To further extend the usefulness of benzimidazoles in organic optoelectronic devices, we postulated a new monomer scaffold, comprising of a 2-(pentafluorophenyl) substituted benzimidazole. Specifically, we expected the weak intramolecular C–F⋯H–N interaction between the benzimidazole NH and the *ortho* fluorines of the pentafluorophenyl to limit the torsion between the two arenes. Computational studies at the DFT RB3LYP/631-G(d) level of theory supported the idea that both arenes would indeed be almost coplanar (see Fig. 1). This coplanarity can lead to extended *p* delocalization and thus a reduction of the HOMO–LUMO gap which, in addition, is stabilized by the electron withdrawing effect of the fluorines. Consequently, 2-(2,3,4,5,6-pentafluorophenyl)-1*H*-benzo[*d*]imidazole (**1**, PFBZ) was an attractive building block for the synthesis of new organic fluorine semiconductors.

In this work we synthesized the 4,7-dibromo-2-(2,3,4,5,6-pentafluorophenyl)-1*H*-benzo[*d*]imidazole (**2**, Br-PFBZ) and its thiophene derivatives (**3**, TPFBZT and **4**, Br-PFBZT, Scheme 1). In addition, the optical and electrochemical properties of these materials were investigated and compared with those of benzo[1,2,5]thiadiazole, the D–A–D thiophene–benzo[1,2,5]thiadiazole–thiophene (TBZT) segment and the well-studied D–A polyfluorene copolymer APFO-3.^{35,36}

Results and discussion

Monomer and polymer synthesis

The reaction of 2,3,4,5,6-pentafluorobenzaldehyde with readily prepared 3,6-dibromobenzene-1,2-diamine³⁷ in the presence of *p*-toluenesulfonic acid (*p*-TsOH) as the organocatalyst in dimethylformamide (DMF), gave the dibromo-PFBZ derivative **2** in moderate yields (Scheme 1). The synthesis of the dithienylbenzimidazole **3** was achieved in moderate yields by the Stille cross-coupling reaction between the dibromobenzimidazole **2** and 2-(tributylstannyl)thiophene using tetrakis(tri-phenylphosphine) palladium [Pd(Ph₃P)₄] (5 mol%) as the catalyst. Bromination of the dithiophene **3** was subsequently carried out using *N*-bromosuccinimide (NBS) in DMF, providing the di(bromothiophene) **4** as a yellow–green fluorescent solid.

To compare the optical and electrochemical properties of the synthesized monomers Br-PFBZ and TPFBZT, the D–A–D thiophene–benzo[1,2,5]thiadiazole–thiophene (TBZT) segment was also synthesized according to literature procedures.³⁸

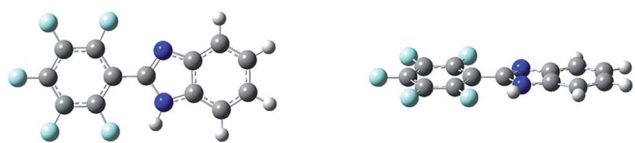


Fig. 1 Optimized structure of 2-(2,3,4,5,6-pentafluoro-phenyl)-1*H*-benzo[*d*]imidazole (**1**, PFBZ) (top and side views) at the DFT RB3LYP/6-31G(d) level of theory.

Polyfluorene copolymers are the most popular group of materials for various optoelectronic applications, due not only to their easy processing and excellent optoelectronic properties but also due to the commercial availability of the diboronic dialkylated fluorene derivative. Taking this into account, a PFBZ-based polyfluorene copolymer PFTPFBZT was synthesized (Scheme 2) by the copolymerization of a diboronic bis(2-ethylhexyl)-fluorene with the di(bromothiophene) **4** by the Suzuki cross-coupling reaction, using Pd(Ph₃P)₄ as the catalyst and (2 M) aq. K₂CO₃ as the base in DMF. The polymerization was run at *ca.* 100 °C under an argon atmosphere for 72 h. After purification using Soxhlet extraction and according to size-exclusion chromatography (SEC) experiments based on monodisperse polystyrene standards, the chloroform fraction has a molecular weight of $M_w = 3.1 \text{ kg mol}^{-1}$ and a PDI of 1.54. Since the experimental parameter of molecular weight plays a crucial role in device performance,^{39,40} the APFO-3 sample was also examined, and exhibited an M_n of 5000 ($M_w = 10\,000$). The polymer PFTPFBZT shows excellent thermal stability (5% of weight loss at 350 °C) and is completely soluble in tetrahydrofuran (THF) and chlorinated solvents such as dichloromethane (DCM), chloroform and chlorobenzene.

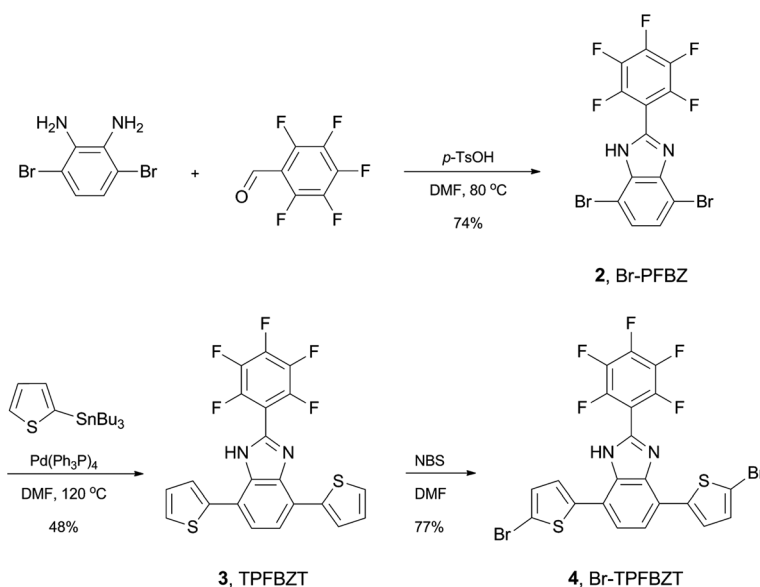
Optical characterization

The optical characterization of the synthesized materials took place both in solution and in the solid state. Since the synthesized polymer shares a structural resemblance to the APFO-3 copolymer, the building blocks and the polymers were examined side-by-side to help elucidate the effect of the fluorinated benzimidazole *vs.* the benzothiadiazole units, both as stand-alone units and when forming donor–acceptor–donor (D–A–D) triads with thiophene.

When examining the Br-PFBZ in DCM (Fig. 2), a single absorption peak at 298 nm is seen. The peak is slightly blue-shifted compared to the benzothiadiazole's absorption at 308 nm. Upon synthesizing the D–A–D triads the optical characteristics change. The main absorption of the thiophene–benzothiadiazole–thiophene triad appears at 279 nm, blue-shifted compared to the pristine benzothiadiazole, while a weaker peak at lower energies (447 nm) appears. On the other hand, the fluorinated benzimidazole, when coupled to thiophene, (TPFBZT) exhibits its main absorption at longer wavelengths *i.e.* at 340 nm with a weaker, blue-shifted peak at 260 nm compared to benzothiadiazole.

The polymer PFTPFBZT in solution and thin film exhibits single absorption peaks at 431 and 451 nm, respectively. In contrast, the APFO-3 spectrum shows two well-resolved peaks at 383 and 530 nm. The two-peak absorption is typically considered as an optical signature of a successful push–pull molecule interaction^{41,42} exhibiting intramolecular charge transfer. The single-peaked spectrum and the relatively large optical bandgap of 2.25 eV of PFTPFBZT indicate a rather unsuccessful application of the donor–acceptor approach. Furthermore, when compared to established light harvesting polymers such as regioregular RR-P3HT and APFO-3, the newly synthesized PFTPFBZT shows a lower absorption coefficient by a factor of ~ 2 (Fig. 3).

The emission of the fluorinated polymer when resonantly excited to the peak of the absorption (450 nm) exhibits a single broad peak at 575 nm (Fig. 4a). The spectrum contains visible vibronics equidistant in energy by $\sim 0.11 \text{ eV}$. When blended with



Scheme 1 Synthetic route to the pentafluorophenyl monomer 4 (Br-TPFBZ).

[6,6]-phenyl C61 butyric acid methyl ester (PCBM) in a 1 : 3 blend, a highly efficient polymer emission quenching (~two orders of magnitude) was observed. The weak remnant blend emission does not originate from the conjugated polymer under study, but comes almost exclusively from the PCBM component. As seen on the normalized spectra (Fig. S6, ESI[†]), the blend emission contains fluorescence due to the singlet PCBM exciton at wavelengths larger than 700 nm, while a higher energy band at 510–530 nm is visible for both PCBM and the blend. Bradley *et al.*⁴³ have attributed the emission that appears at the film regions of high concentration in PCBM to the inter-chain charge transfer of fullerene excitons.

Fluorescence lifetime measurements (Fig. 4) were conducted on the PFTPFBZT conjugated polymer. The material was excited at 375 nm (3.31 eV) and the time evolution of the fluorescence was monitored using a time-correlated single photon counting (TCSPC) system (~50 ps time resolution). The decays

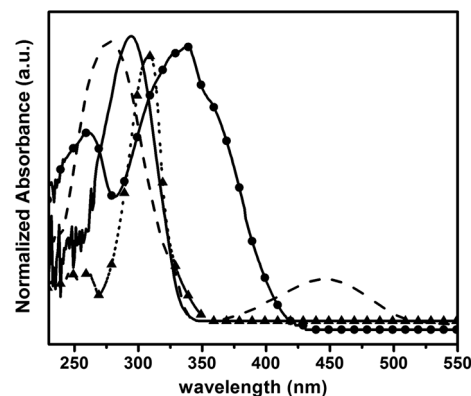
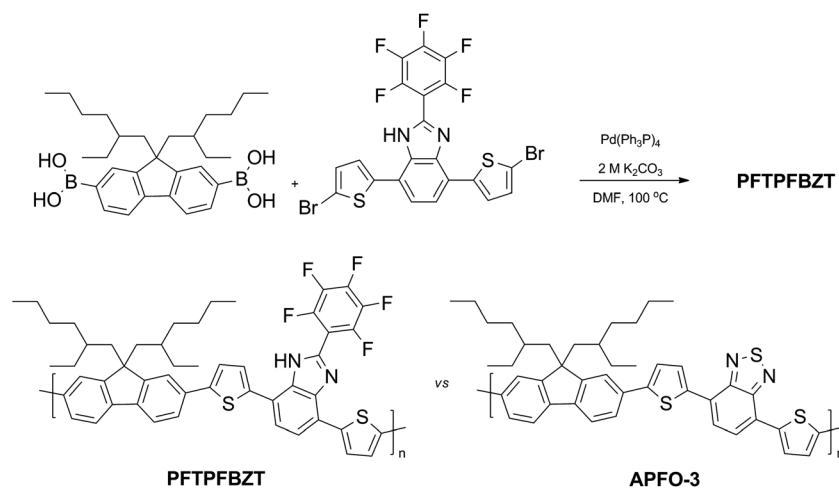


Fig. 2 Absorption spectra in DCM of the monomers Br-PFBZ (solid line) and TPFBZT (-●-) in comparison to the APFO-3 building blocks of benzo[1,2,5]thiadiazole (-▲-) and thiophene-benzothiadiazole-thiophene (dashed line).



Scheme 2 Synthetic route to the polymer PFTPFBZT.

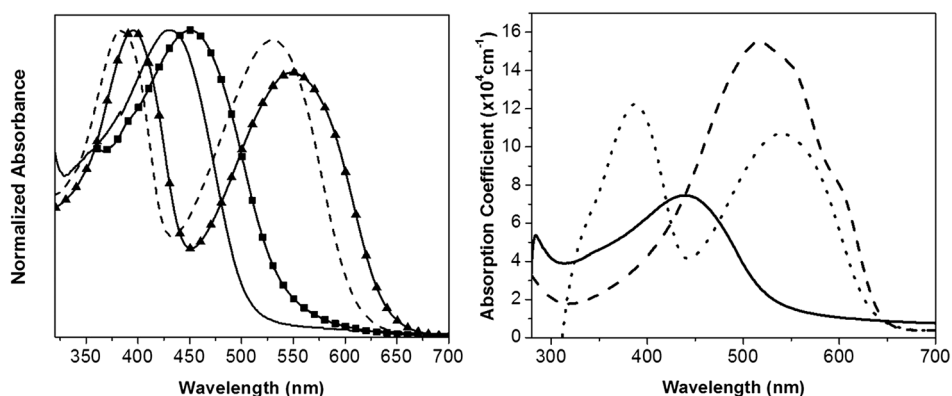


Fig. 3 Normalized absorption spectra (left) of PFTPFBZ in DCM (solid line) and in solid state (-■-) compared to APFO-3 in DCM (dashed line) and in solid state (-▲-). Absorption coefficient spectra (right) of PFTPFBZ (solid line) compared to RR-P3HT (dashed line) and APFO-3 (dotted line).

at the peaks of 4 different vibronics (550, 578, 608 and 645 nm) were probed (two are shown) and similar kinetics were obtained at all energies. All decays are described by a double exponential model:

$$I(t) = I_1 e^{-t/\tau_1} + I_2 e^{-t/\tau_2}$$

with a fast dominant decay τ_1 in the range of 60–90 ps and a relative amplitude $[I_1/(I_1 + I_2)]$ of 90–95%, and a significantly slower decay τ_2 in the range of 900–1100 ps with a relative amplitude $[I_2/(I_1 + I_2)]$ of 5–10%. The dominant, fast decay is most likely to be due to an efficient non-radiative quenching of the photoexcited excitons while the longer decay can be attributed to the radiative exciton recombination. Based on the above, a rough estimation of 5–10% for the quantum yield of the fluorescence for the PFTPFBZ conjugated polymer can be obtained. The interpretation is further supported by a comparative side-by-side fluorescence study of the PFTPFBZ films with RR-P3HT films of equal thickness. When the films are excited at 440 nm, where both materials exhibit approximately equal absorption coefficients, the integrated emission from the two conjugated polymers under investigation (spectra not shown) is comparable, which indicates a low emission quantum yield of PFTPFBZ, comparable to that observed in the RR-P3HT films ($\sim 2\%$).⁴⁴

Electrochemical characterization

Electrochemical studies on the conjugated polymers under study were performed to elucidate the energy levels and the differentiation induced by the chemical modification. A standard three-electrode cell was used with Ag/AgCl as a reference electrode and a Pt wire and Pt mesh as the working and counter electrodes, respectively. Differential pulse voltammetry was used to minimize the influence of the capacitive current.

Upon electrochemical examination of the synthesized materials (Fig. 5), the dibromopentafluorophenylbenzimidazole Br-PFBZ exhibits a reversible reduction at -1.85 V and an irreversible oxidation procedure at 1.43 V. This yields HOMO and LUMO energy levels of 6.33 and 3.25 eV, respectively. When thiophene was attached to the fluorinated benzimidazole, a sharp electrochemical differentiation was observed. There are two oxidation peaks, one corresponding to irreversible oxidation located at $E_{1/2} = 0.81$ V and one corresponding to reversible oxidation with an $E_{1/2} = 1.12$ V. The reversible behavior can probably be attributed to the thiophene moiety, since the Br-PFBZ did not show similar features when examined. Also, no clear reduction process was witnessed. The HOMO from the onset of the oxidation process was calculated at 5.67 eV, significantly shifted compared to Br-PFBZ. When polymerizing with fluorene, according to the donor–acceptor approach we expected

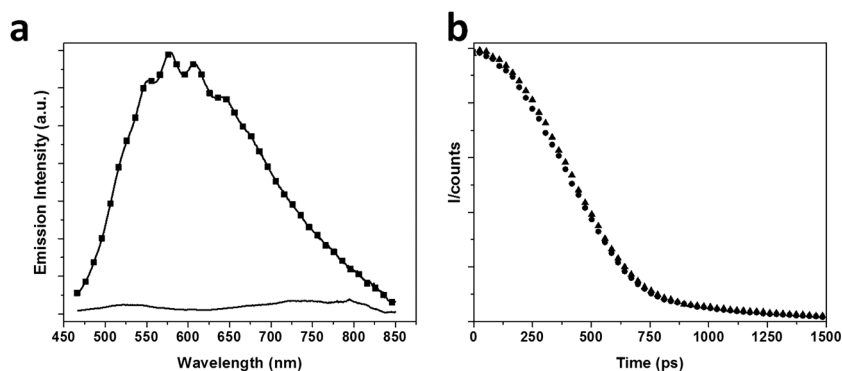


Fig. 4 (a) Emission spectra of PFTPFBZ in the solid state (-■-) and when blended with PCBM (solid line). (b) Fluorescence lifetime decay of PFTPFBZ performed at room temperature, in the solid state, at $\lambda_{em} = 578$ nm (▲) and $\lambda_{em} = 643$ nm (●).

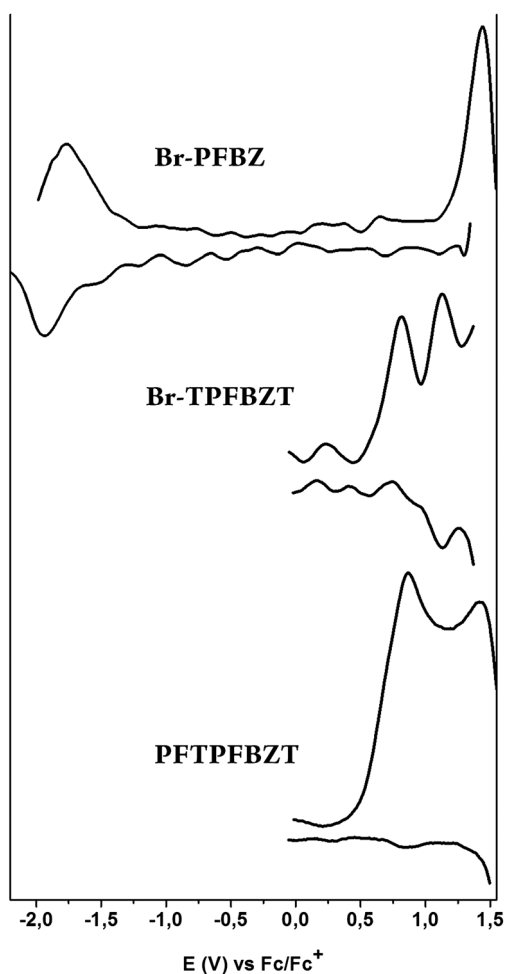


Fig. 5 Differential pulse voltammetry oxidation and reduction runs on Br-PFBZ and Br-TPFBZ in solution (0.1 M TBAPF₆ in DCM) and the copolymer PFTPFBZ in thin film (0.1 M TBAPF₆ in acetonitrile). Step height: 25 mV, step width: 5 mV, pulse height: 50 ms, pulse width: 100 ms. All potentials vs. Fc/Fc⁺.

the characteristic fluorene oxidation peak to be present. This was evident when the commercially available APFO-3 was tested, exhibiting a reversible oxidation at 0.70 V yielding a HOMO of 5.80 eV in good agreement with the values reported by Inganäs and co-workers.^{45,46} However, the synthesized PFTPFBZ more closely resembles the parent Br-TPFBZ molecule, exhibiting two non-reversible oxidations at 0.87 and 1.42 V. The oxidation onset denotes that the calculated HOMO lies at around 5.60 eV. Taking into account the optical bandgap of 2.25 eV (calculated from the UV-vis spectrum), the LUMO of the copolymer lies at around 3.35 eV. We note that in order to synthesize low bandgap polymers following the so-called donor–acceptor approach,^{47,48} special attention has to be paid to the energy levels of the comonomers used. Electrochemical studies of the comonomer Br-TPFBZ reveal that the HOMO of the monomer could not effectively engineer the desirable bandgap of the end-polymer when coupled with fluorene. Electrochemical data, along with the optical data, support the notion that the push–pull intramolecular interaction does not take place in the synthesized polymer and a variation of the acceptor moiety is probably needed to achieve the desired effect.

Photovoltaic performance

The PFTPFBZ conjugated polymer was evaluated in terms of its power conversion efficiency performance on polymer–fullerene bulk heterojunction solar cells relevant to the reference APFO-3–fullerene-based bulk heterojunction solar cells. Fig. 6 summarizes the representative *J–V* characteristics under 100 mW cm⁻² irradiance for organic solar cells using APFO-3–PCBM and PFTPFBZ : PCBM photoactive layers.

The photovoltaic parameters measured at 1.5 A.M. conditions, namely open circuit voltage (*V*_{oc}), short circuit current density (*J*_{sc}), fill factor (FF) and power conversion efficiency (PCE) of the polymer–fullerene-based solar cells under study are summarised in Table 1.

Based on the polymer characteristics and the theoretical model prediction, the PFTPFBZ : PCBM bulk heterojunction organic solar cells can achieve a maximum power conversion efficiency (PCE) in the range of 2.5%. The early investigations on the device performance show that PFTPFBZ : PCBM-based bulk heterojunction solar cells exhibit modest power conversion efficiencies of 0.24% compared to the 1.75% PCE achieved for the reference APFO-3 : PCBM-based bulk heterojunction solar cells. When PFTPFBZ : PCBM was used as the photo-active layer, lower *V*_{oc} values in comparison to devices with APFO-3 : PCBM were obtained. This could be partially explained by the difference in the HOMO of the two fluorene-based copolymers. The *V*_{oc} values achieved are significantly lower than the theoretical maximum potential, indicating possible recombination losses. In combination with the low FF values obtained, the results indicate morphological limitation for both PFTPFBZ : PCBM (1 : 3) and (1 : 4), (w/w) concentrations. The low *J*_{sc} values for PFTPFBZ : PCBM-based solar cells are due in part to the moderate *E*_g of 2.25 eV, which was calculated from the UV-vis spectrum. The modest molecular weights could have also impacted the performance of the devices. However, based on our study, we believe that increasing the molecular weights of our benzimidazole material will not lead to significantly superior

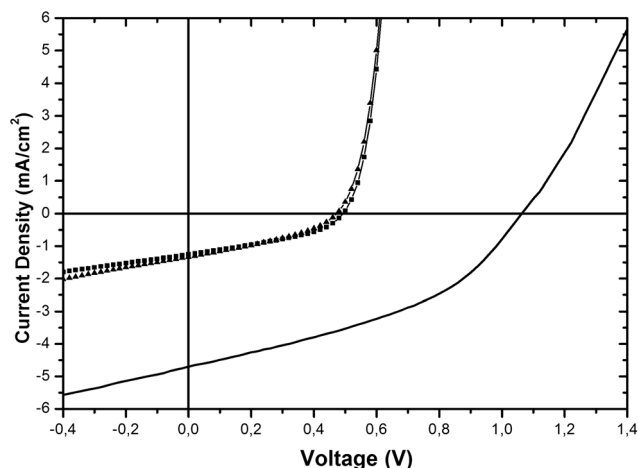


Fig. 6 *J–V* characteristics under illumination of organic photovoltaic devices based on PFTPFBZ : PCBM at 1 : 3 (–▲–) and 1 : 4 (–■–) ratio compositions by weight (w/w) and compared with APFO-3 : PCBM (solid line) 1 : 4 (w/w) that was used as reference organic solar cell device system.

Table 1 Summary of the photovoltaic parameters acquired from illuminated J - V device characteristics

Blend	V_{oc} (V)	J_{sc} (mA cm ⁻²)	FF (%)	PCE (%)
APFO-3 : PCBM (1 : 4)	0.96	4.49	40.5	1.75
PFTPFBZT : PCBM (1 : 3)	0.47	1.33	36	0.22
PFTPFBZT : PCBM (1 : 4)	0.49	1.25	38.8	0.24

properties for the photovoltaic devices reported. The fabricated photovoltaic devices reported provide an initial photovoltaic loss analysis for the PFTPFBZT : PCBM-based solar cells and serve as a guideline for comparison to well-established polymers with structural similarities. In summary, the initial investigations suggest that morphological limitations and moderate E_g are the main factors limiting the PCE of PFTPFBZT : PCBM-based solar cells compared to other high performance conjugated polymer–fullerene-based material systems.

Experimental

Computational procedure

The geometry of 2-(2,3,4,5,6-pentafluorophenyl)-1H-benzo[d]imidazole (PFBZ) was fully optimized and analytical second derivatives were computed using vibrational analysis to confirm each stationary point to be a minimum by yielding zero imaginary frequencies at the DFT RB3LYP/6-31G(d) level of theory.^{49,50} The possibility of internal instability in the singlet wave function was investigated using stability calculations. All the above computations were performed using the Gaussian 03 suite of programs.⁵¹

Instrumentation

Melting points were determined using a TA Instruments DSC Q1000 with samples hermetically sealed in aluminium pans under an argon atmosphere using heating rates of 5 °C min⁻¹, and are defined by their onset and peak temperatures. ¹H NMR spectra were recorded on a Bruker Avance 500 machine at 500 MHz. Deuterated solvents were used for homonuclear lock and the signals are referenced to the deuterated solvent peaks. Low resolution (EI) mass spectra were recorded on a Shimadzu Q2010 GC-MS with a direct inlet probe. Microanalysis was performed at London Metropolitan University on a Perkin Elmer 2400 Series II CHN Analyzer.

Number-average (M_n) and weight-average (M_w) were determined by Agilent Technologies 1200 series GPC running in chlorobenzene at 80 °C, using two PL mixed B columns in series, and calibrated against narrow polydispersity polystyrene standards.

Film absorption was carried out on a Lambda 1050 UV-vis/NIR spectrophotometer (Perkin Elmer). Steady-state and time-resolved fluorescence were measured on a NanoLog FL3 spectrofluorometer (Horiba Jobin Yvon). Steady-state spectra were excited by an Ozone-free 450 W Xenon Lamp. Time-resolved fluorescence was measured by the time-correlated single-photon counting (TCSPC) method using a picosecond laser diode as an excitation source (NanoLED, 375 nm). The system exhibits a time-resolution of 50 ps after reconvolution with the laser

excitation pulses using the DAS6 (Horiba Jobin Yvon) software analysis package.

Cyclic voltammetry studies were performed using a standard three-electrode cell under argon atmosphere. All measurements were performed with Ar bubbling into the electrochemical cell for 15 min. 10 s prior to the measurements the Ar was turned to “blanket mode”. Platinum wire (99.99%) was used as working electrode and platinum gauze (55 mesh, 99.9%) as counter electrode. Ag/AgCl was used as a reference electrode. Tetrabutylammonium hexafluorophosphate (TBAPF₆, 98%) was used as the electrolyte and was recrystallized three times from acetone and dried in vacuum at *ca.* 100 °C before each experiment. Measurements were recorded using an EG&G Princeton Applied Research potentiostat/galvanostat Model Verstatat 4 connected to a personal computer running VersaStudio software. The scan rate was kept constant for all CV runs at 100 mV s⁻¹, while for differential pulse voltammetry measurements, the following parameters were used: step height 25 mV; step width 5 mV; pulse height 50 ms and pulse width 100 ms. All the results were calibrated using commercially available ferrocene (purified by sublimation) as an internal standard. All the polymer samples were studied in the solid state by forming a thin film on the working electrode from a viscous DCM solution of the polymer and subsequent drying of the electrode. To calculate HOMO/LUMO levels using the potentials obtained, the following equations⁵² were used

$$E_{\text{HOMO}} = -(E[\text{ox vs. Fc/Fc}^+] + 5.1) \text{ (eV)}$$

$$E_{\text{LUMO}} = -(E[\text{red vs. Fc/Fc}^+] + 5.1) \text{ (eV)}$$

When a reversible process was observed, the $E_{1/2}$ was considered, whereas in a non-reversible process the onset of the peak was used in the calculation.

For device preparation, pre-patterned ITO substrates were cleaned primarily with acetone and then with isopropanol in an ultra sonic bath for 10 min. Afterwards a thin layer of PEDOT/PSS (Clevios™ PH) was doctor bladed on top with a measured thickness of 50 nm. Thermal annealing of the deposited layer was performed to ensure the removal of any residual solvent from the deposited film. On top of that, the optically active layer consisted of APFO-3 and PFTPFBZT blended with PCBM at different ratios in each case was deposited. Polymers and PCBM were separately diluted overnight in chlorobenzene at 70 °C and were mixed 1 h prior to deposition. Various parameters were used to achieve an average thickness of 70 nm for both layers. Thickness measurements, performed with a Veeco profilometer, were followed by thermal deposition of a bi-metal cathode, which consisted of 1 nm of LiF and 80 nm of Al. The effective photovoltaic area was defined by the geometrical overlapping between the anode and cathode and was measured to be 9 mm². A Keithley 2420 source meter recorded the current density vs. voltage (J - V) characteristics under 100 mW cm⁻² irradiance and at 1.5 A.M. conditions with a Newport solar simulator.

Materials

Toluene was distilled from metallic sodium and benzophenone, DMF was distilled with calcium chloride and NBS was

recrystallized (H₂O) prior to use. All the other solvents and reagents were obtained from Aldrich and were used without further purification. APFO-3 was purchased from Luminescence Technology Corporation and used without further purification. Tetrakis(triphenylphosphine)palladium [Pd(Ph₃P)₄]⁵³ and 3,6-dibromobenzene-1,2-diamine³⁷ were synthesized according to literature procedures.

Monomer synthesis

4,7-Dibromo-2-(2,3,4,5,6-pentafluorophenyl)-1H-benzo-[d]imidazole (2). 2,3,4,5,6-Pentafluorobenzaldehyde (500.0 mg, 2.55 mmol) and 3,6-dibromobenzene-1,2-diamine (678.3 mg, 2.55 mmol) were thoroughly mixed in DMF (10 mL), then *p*-TsOH (97 mg, 0.51 mmol) was added and the stirred solution was then heated at *ca.* 80 °C for 45 min (monitored by TLC). On completion, the reaction mixture was allowed to cool to *ca.* 20 °C and then added dropwise into a vigorously stirred 0.05 M aq. Na₂CO₃ (100 mL). The precipitate that formed was collected by filtration, washed (H₂O) and dried. Column chromatography over silica gel (cyclohexane–EtOAc, 3 : 1) afforded compound **2** (0.76 g, 74%). Mp (DSC) onset: 317.55 °C, peak: 318.86 °C. Elemental analysis found: C, 35.23; H, 0.61; N, 6.27%. Calc. for C₁₃H₃Br₂F₅N₂: C, 35.33; H, 0.68; N, 6.34%. ¹H NMR (500 MHz, DMSO-*d*₆, ppm): δ_H = 8.40 (s, 1H), 7.38 (s, 2H). *m/z* (EI) 444 (M⁺ + 4, 51%), 442 (M⁺ + 2, 100), 440 (M⁺, 51), 363 (11), 361 (11), 278 (32), 276 (70), 274 (36), 221 (13), 197 (14), 195 (15), 170 (18), 168 (21), 116 (31), 89 (40), 62 (38), 52 (8).

2-(2,3,4,5,6-Pentafluorophenyl)-4,7-di(thien-2-yl)-1H-benzo[d]imidazole (3). 2-(Tributylstannyl)thiophene (1.58 g, 4.24 mmol) and 4,7-dibromo-2-(2,3,4,5,6-pentafluorophenyl)-1H-benzo[d]imidazole (**2**) (0.75 g, 1.69 mmol) were dissolved in dry toluene (18 mL). Then, Pd(Ph₃P)₄ (9.80 mg, 5 mol%) was added and the stirred reaction mixture was heated at *ca.* 110 °C for 1 day under an argon atmosphere. On cooling to *ca.* 20 °C, the reaction mixture was filtered (celite) and the volatiles were removed *in vacuo*. The residue was washed (EtOH), filtered and then recrystallized (from cyclohexane) to give compound **3** as a yellow solid (0.91 g, 48%). Mp (DSC) onset: 203.20 °C, peak: 224.69 °C (decomp.). Elemental analysis found: C, 56.17; H, 2.00; N, 6.23%. Calc. for C₂₁H₉F₅N₂S₂: C, 56.25; H, 2.02; N, 6.25%. ¹H NMR (500 MHz, CDCl₃, ppm): δ_H = 10.10 (s, 1H), 8.24 (s, 1H), 7.67 (d, 1H), 7.64 (d, 1H), 7.45–7.39 (m, 3H), 7.22–7.20 (m, 2H). *m/z* (EI) 448 (M⁺, 100%), 403 (8), 282 (69), 237 (12), 224 (14), 209 (5), 202 (9), 141 (8), 119 (6), 69 (5).

4,7-Bis(5-bromothiien-2-yl)-2-(2,3,4,5,6-pentafluoro-phenyl)-1H-benzo[d]imidazole (4). 2-(2,3,4,5,6-Pentafluoro-phenyl)-4,7-di(thien-2-yl)-1H-benzo[d]imidazole (**3**) (0.45 g, 0.65 mmol) was dissolved in DMF (15 mL) under argon in the dark and NBS (0.268 g, 1.51 mmol) was added portion-wise. The resulting solution was stirred at *ca.* 20 °C under argon for an additional 2 h. Then, it was extracted (EtOAc) and the organic phase washed with KOH (10 wt%) and water, then dried (Na₂SO₄). The volatiles were then removed *in vacuo* and recrystallization (from acetone) of the residue gave compound **4** as a yellow–green solid (0.30 g, 77%). Mp (DSC) onset: 189.18 °C, peak: 191.33 °C. Elemental analysis found: C, 41.57; H, 1.01; N, 4.52%. Calc. for

C₂₁H₇Br₂F₅N₂S₂: C, 41.61; H, 1.16; N, 4.62%. ¹H NMR (500 MHz, CDCl₃, ppm): δ_H = 9.88 (s, 1H), 8.17 (s, 1H), 7.55 (d, 1H), 7.46–7.41 (m, 2H), 7.16–7.11 (m, 2H). *m/z* (EI) 608 (M⁺ + 4, 59%), 606 (M⁺ + 2, 100), 604 (M⁺, 50), 528 (13), 526 (14), 446 (12), 442 (42), 440 (80), 438 (39), 414 (22), 360 (13), 303 (12), 280 (28), 235 (17), 223 (27), 209 (10), 179 (15), 164 (13), 140 (38), 118 (20), 104 (13), 91 (11), 69 (15).

Polymer synthesis (PFTFPBZT)

In a carefully degassed flask, diboronic bis(2-ethylhexyl)-fluorene (173 mg, 0.36 mmol) and 4,7-dibromo-2-(2,3,4,5,6-pentafluorophenyl)-1H-benzo[d]imidazole (**6**) (220 mg, 0.36 mmol) along with Pd(Ph₃P)₄ (21 mg, 5 mol%) were mixed. Deaerated DMF (20 mL) and 2 M aq. K₂CO₃ (3 mL) were added and the mixture was heated to *ca.* 120 °C and stirred for 3 days. The mixture was then allowed to cool to *ca.* 20 °C, filtered to remove the catalyst, and then EtOAc (100 mL) and H₂O (30 mL) were added. The mixture was washed (EtOAc, 3 × 100 mL) and the organic layer was separated, dried (Na₂SO₄) and concentrated *in vacuo*. Purification using Soxhlet extraction with MeOH (200 mL) for 1 day, then hexane (200 mL) for 1 day and finally with CHCl₃ (200 mL) for 1 day afforded the higher *M_w* fraction (70.6 mg). ¹H NMR (500 MHz, CDCl₃, ppm): δ_H = 7.83–7.39 (br m, 12H), 3.32–2.94 (m, 6H), 2.11, 2.04 (m, 8H), 1.67 (br m, 4H), 0.88–0.56 (br m, 16H).

Conclusions

A novel polymer bearing the pentafluorophenyl moiety as a side chain has been synthesized. The aim was to produce a strong acceptor monomer owing to the presence of multiple fluorine atoms. The idea of creating D–A–D triads with a thiophene moiety prior to polymerization was used to increase the intramolecular interaction. Upon copolymerization with fluorene *via* Suzuki coupling, a copolymer with a relatively high bandgap of 2.25 eV was obtained. Optical and electrochemical characterization strengthened the notion that intramolecular interactions probably did not take place, resulting in a minimal lowering of the energy bandgap. Efficient quenching of the polymer emission within a blend with PCBM indicates, however, the presence of a fast exciton dissociation at the polymer–fullerene hetero-interfaces. Photovoltaic efficiency measurements were carried out with PC₆₀BM and showed a power conversion efficiency of 0.24%, compared to 1.75% for the APFO-3 : PCBM-based devices, indicating that in addition to the unfavorable bandgap, there are morphological limitations. Synthetic attempts at using the pentafluorophenyl moiety as a building block whilst optimizing the side chains, aiming at improved solubility and hopefully shifting the energy levels to more favorable values, are currently under way to achieve higher power conversion efficiency values.

Acknowledgements

Munazza Shahid, of Imperial College, London is acknowledged for his aid in obtaining the GPC data. This work was co-funded by the European Regional Development Fund and the Republic of Cyprus through the Research Promotion Foundation (Strategic Infrastructure Project NEA YΠOΔOMH/ΣTPATH/0308/06

and the following organizations in Cyprus for generous donations of chemicals and glassware: the State General Laboratory, the Agricultural Research Institute, the Ministry of Agriculture and Bionics Ltd. Furthermore, we thank the A.G. Leventis Foundation for helping to establish the NMR facility in the University of Cyprus.

Notes and references

- N. S. Sariciftci, L. Smilowitz, A. J. Heeger and F. Wudl, *Science*, 1992, **258**, 1474–1476.
- S. C. Price, A. C. Stuart, L. Yang, H. Zhou and W. You, *J. Am. Chem. Soc.*, 2011, **133**, 4625–4631.
- Y. Liang, Z. Xu, J. Xia, S.-T. Tsai, Y. Wu, G. Li, C. Ray and L. Yu, *Adv. Mater.*, 2010, **22**, E135–E138.
- L. Huo, S. Zhang, X. Guo, F. Xu, Y. Li and J. Hou, *Angew. Chem., Int. Ed.*, 2011, **50**, 9697–9702.
- H.-Y. Chen, J. Hou, S. Zhang, Y. Liang, G. Yang, Y. Yang, L. Yu, Y. Wu and G. Li, *Nat. Photonics*, 2009, **3**, 649–653.
- <http://www.polyera.com/newsflash/polyera-achieves-world-record-organic-solar-cell-performance>.
- J. C. Hummelen, B. W. Knight, F. LePeq, F. Wudl, J. Yao and C. L. Wilkins, *J. Org. Chem.*, 1995, **60**, 532–538.
- M. M. Wienk, J. M. Kroon, W. J. H. Verhees, J. Knol, J. C. Hummelen, P. A. van Hal and R. A. J. Janssen, *Angew. Chem., Int. Ed.*, 2003, **42**, 3371–3375.
- F. B. Kooistra, V. D. Mihailetschi, L. M. Popescu, D. Kronholm, P. W. M. Blom and J. C. Hummelen, *Chem. Mater.*, 2006, **18**, 3068–3073.
- E. H. Sargent, *Nat. Photonics*, 2009, **3**, 325–331.
- P. Kirsch, in *Modern Fluoroorganic Chemistry*, Wiley-VCH Verlag GmbH & Co. KGaA, 2005, pp. 25–169.
- M. Steenackers, A. M. Gigler, N. Zhang, F. Deubel, M. Seifert, L. H. Hess, C. H. Y. X. Lim, K. P. Loh, J. A. Garrido, R. Jordan, M. Stutzmann and I. D. Sharp, *J. Am. Chem. Soc.*, 2011, **133**, 10490–10498.
- M. Pagliaro and R. Ciriminna, *J. Mater. Chem.*, 2005, **15**, 4981.
- H. Behniafar and M. Sedaghatdoost, *J. Fluorine Chem.*, 2011, **132**, 276–284.
- A. A. Stefopoulos, S. N. Kourkouli, S. Economopoulos, F. Ravani, A. Andreopoulou, K. Papagelis, A. Siokou and J. K. Kallitsis, *Macromolecules*, 2010, **43**, 4827–4828.
- J. T. Robinson, J. S. Burgess, C. E. Junkermeier, S. C. Badescu, T. L. Reinecke, F. K. Perkins, M. K. Zalalutdniov, J. W. Baldwin, J. C. Culbertson, P. E. Sheehan and E. S. Snow, *Nano Lett.*, 2010, **10**, 3001–3005.
- K.-J. Jeon, Z. Lee, E. Pollak, L. Moreschini, A. Bostwick, C.-M. Park, R. Mendelsberg, V. Radmilovic, R. Kostecki, T. J. Richardson and E. Rotenberg, *ACS Nano*, 2011, **5**, 1042–1046.
- S. Wong, H. Ma, A. K. Y. Jen, R. Barto and C. W. Frank, *Macromolecules*, 2003, **36**, 8001–8007.
- K. Reichenbacher, H. I. Suss and J. Hulliger, *Chem. Soc. Rev.*, 2005, **34**, 22.
- S. B. Heidenhain, Y. Sakamoto, T. Suzuki, A. Miura, H. Fujikawa, T. Mori, S. Tokito and Y. Taga, *J. Am. Chem. Soc.*, 2000, **122**, 10240–10241.
- F. Babudri, G. M. Farinola, F. Naso and R. Ragni, *Chem. Commun.*, 2007, 1003–1022.
- A. Facchetti, M.-H. Yoon, C. L. Stern, H. E. Katz and T. J. Marks, *Angew. Chem.*, 2003, **115**, 4030–4033.
- J. H. Oh, S. L. Suraru, W.-Y. Lee, M. Könemann, H. W. Höffken, C. Röger, R. Schmidt, Y. Chung, W.-C. Chen, F. Würthner and Z. Bao, *Adv. Funct. Mater.*, 2010, **20**, 2148–2156.
- M.-H. Yoon, S. A. DiBenedetto, A. Facchetti and T. J. Marks, *J. Am. Chem. Soc.*, 2005, **127**, 1348–1349.
- J. D. Yuen, J. Fan, J. Seifert, B. Lim, R. Hufschmid, A. J. Heeger and F. Wudl, *J. Am. Chem. Soc.*, 2011, **133**, 20799–20807.
- H. Zhou, L. Yang, S. Stoneking and W. You, *ACS Appl. Mater. Interfaces*, 2010, **2**, 1377–1383.
- H. Zhou, L. Yang, S. C. Price, K. J. Knight and W. You, *Angew. Chem., Int. Ed.*, 2010, **49**, 7992–7995.
- H. Zhou, L. Yang, A. C. Stuart, S. C. Price, S. Liu and W. You, *Angew. Chem., Int. Ed.*, 2011, **50**, 2995–2998.
- J. S. Kim, Y. Lee, J. H. Lee, J. H. Park, J. K. Kim and K. Cho, *Adv. Mater.*, 2010, **22**, 1355–1360.
- Y. Liang, D. Feng, Y. Wu, S.-T. Tsai, G. Li, C. Ray and L. Yu, *J. Am. Chem. Soc.*, 2009, **131**, 7792–7799.
- H. Akpınar, A. Balan, D. Baran, E. K. Ünver and L. Toppare, *Polymer*, 2010, **51**, 6123–6131.
- S. Song, Y. Jin, S. H. Park, S. Cho, I. Kim, K. Lee, A. J. Heeger and H. Suh, *J. Mater. Chem.*, 2010, **20**, 6517–6523.
- H. Hayashi and T. Yamamoto, *Macromolecules*, 1998, **31**, 6063–6070.
- H. Zhu, H. Tong, Y. Gong, S. Shao, C. Deng, W. Z. Yuan and Y. Zhang, *J. Polym. Sci., Part A: Polym. Chem.*, 2012, **50**, 2172.
- S. Inganäs, F. Zhang and M. R. Andersson, *Acc. Chem. Res.*, 2009, **42**, 1731–1739.
- H. M. P. Wong, P. Wang, A. Abruci, M. Svensson, M. R. Andersson and N. C. Greenham, *J. Phys. Chem. C*, 2007, **111**, 5244–5249.
- M. J. Edelmann, J.-M. Raimundo, N. F. Utesch, F. Diederich, C. Boudon, J.-P. Gisselbrecht and M. Gross, *Helv. Chim. Acta*, 2002, **85**, 2195–2213.
- A. J. Moulé, A. Tsami, T. W. Bünnagel, M. Forster, N. M. Kronenberg, M. Scharber, M. Koppe, M. Morana, C. J. Brabec, K. Meerholz and U. Scherf, *Chem. Mater.*, 2008, **20**, 4045–4050.
- A. L. Mattias, *Org. Electron.*, 2011, **12**, 300–305.
- L. M. Andersson, C. Muller, B. H. Badada, F. Zhang, U. Würfel and O. Inganäs, *J. Appl. Phys.*, 2011, **110**, 024509.
- M.-H. Chen, J. Hou, Z. Hong, G. Yang, S. Sista, L.-M. Chen and Y. Yang, *Adv. Mater.*, 2009, **21**, 4238–4242.
- P. M. Beaujuge, S. Ellinger and J. R. Reynolds, *Nat. Mater.*, 2008, **7**, 795–799.
- S. Cook, H. Ohkita, Y. Kim, J. J. Benson-Smith, D. D. C. Bradley and J. R. Durrant, *Chem. Phys. Lett.*, 2007, **445**, 276–280.
- S. Cook, A. Furube and R. Katoh, *Energy Environ. Sci.*, 2008, **1**, 294–299.
- L. M. Andersson and O. Inganäs, *Appl. Phys. Lett.*, 2006, **88**, 082103.
- L. M. Andersson, F. Zhang and O. Inganäs, *Appl. Phys. Lett.*, 2007, **91**, 071108.
- H. A. M. van Mullekom, J. A. J. M. Vekemans, E. E. Havinga and E. W. Meijer, *Mater. Sci. Eng., R*, 2001, **32**, 1–40.
- J. Roncali, *Chem. Rev. (Washington, DC, USA)*, 1997, **97**, 173–206.
- C. Lee, W. Yang and R. G. Parr, *Phys. Rev. B*, 1988, **37**, 785–789.
- A. D. Becke, *J. Chem. Phys.*, 1993, **98**, 5648–5652.
- M. J. Frisch, G. W. Trucks, H. B. Schlegel, G. E. Scuseria, M. A. Robb, J. R. Cheeseman, J. A. Montgomery, T. Vreven, K. N. Kudin, J. C. Burant, J. M. Millam, S. S. Iyengar, J. Tomasi, V. Barone, B. Mennucci, M. Cossi, G. Scalmani, N. Rega, G. A. Petersson, H. Nakatsuji, M. Hada, M. Ehara, K. Toyota, R. Fukuda, J. Hasegawa, M. Ishida, T. Nakajima, Y. Honda, O. Kitao, H. Nakai, M. Klene, X. Li, J. E. Knox, H. P. Hratchian, J. B. Cross, V. Bakken, C. Adamo, J. Jaramillo, R. Gomperts, R. E. Stratmann, O. Yazyev, A. J. Austin, R. Cammi, C. Pomelli, J. W. Ochterski, P. Y. Ayala, K. Morokuma, G. A. Voth, P. Salvador, J. J. Dannenberg, V. G. Zakrzewski, S. Dapprich, A. D. Daniels, M. C. Strain, O. Farkas, D. K. Malick, A. D. Rabuck, K. Raghavachari, J. B. Foresman, J. V. Ortiz, Q. Cui, A. G. Baboul, S. Clifford, J. Cioslowski, B. B. Stefanov, G. Liu, A. Liashenko, P. Piskorz, I. Komaromi, R. L. Martin, D. J. Fox, T. Keith, A. Laham, C. Y. Peng, A. Nanayakkara, M. Challacombe, P. M. W. Gill, B. Johnson, W. Chen, M. W. Wong, C. Gonzalez and J. A. Pople, *Gaussian 03, Revision C.02*, Gaussian, Inc., Wallingford, CT, 2004.
- C. M. Cardona, W. Li, A. E. Kaifer, D. Stockdale and G. C. Bazan, *Adv. Mater.*, 2011, **23**, 2367–2371.
- D. R. Coulson, L. C. Satek and S. O. Grim, in *Inorganic Syntheses*, John Wiley & Sons, Inc., 2007, pp. 121–124.